Cell

MicroRNAs Inhibit the Translation of Target mRNAs on the Endoplasmic Reticulum in *Arabidopsis*

Shengben Li,[1] Lin Liu,[1,3] Xiaohong Zhuang,[4] Yu Yu,[1,5] Xigang Liu,[1] Xia Cui,[6] Lijuan Ji,[1] Zhiqiang Pan,[7] Xiaofeng Cao,[6] Beixin Mo,[5] Fuchun Zhang,[3] Natasha Raikhel,[1] Liwen Jiang,[4] and Xuemei Chen[1,2,*]

[1]Department of Botany and Plant Sciences, Institute of Integrative Genome Biology
[2]Howard Hughes Medical Institute
University of California, Riverside, Riverside, CA 92521
[3]Xinjiang Key Laboratory of Biological Resources and Genetic Engineering, College of Life Science and Technology, Xinjiang University, Urumqi 830046, China
[4]School of Life Sciences, Centre for Cell and Developmental Biology, Chinese University of Hong Kong, Shatin, New Territories, Hong Kong, China
[5]Shenzhen Key Laboratory of Microbial Genetic Engineering, College of Life Sciences, Shenzhen University, Shenzhen 518060, China
[6]Institute of Genetics and Developmental Biology, Chinese Academy of Sciences, Beijing 100101, China
[7]Agricultural Research Service, United States Department of Agriculture, University of Mississippi, University, MS 38677
*Correspondence: xuemei.chen@ucr.edu
http://dx.doi.org/10.1016/j.cell.2013.04.005

SUMMARY

Translation inhibition is a major but poorly understood mode of action of microRNAs (miRNAs) in plants and animals. In particular, the subcellular location where this process takes place is unknown. Here, we show that the translation inhibition, but not the mRNA cleavage activity, of *Arabidopsis* miRNAs requires *ALTERED MERISTEM PROGRAM1* (*AMP1*). *AMP1* encodes an integral membrane protein associated with endoplasmic reticulum (ER) and ARGONAUTE1, the miRNA effector and a peripheral ER membrane protein. Large differences in polysome association of miRNA target RNAs are found between wild-type and the *amp1* mutant for membrane-bound, but not total, polysomes. This, together with *AMP1*-independent recruitment of miRNA target transcripts to membrane fractions, shows that miRNAs inhibit the translation of target RNAs on the ER. This study demonstrates that translation inhibition is an important activity of plant miRNAs, reveals the subcellular location of this activity, and uncovers a previously unknown function of the ER.

INTRODUCTION

microRNAs (miRNAs) are ~21 nucleotide (nt) small RNAs that impact numerous biological processes in diverse eukaryotes. miRNAs repress target gene expression in two main manners, mRNA degradation and translation inhibition. mRNA degradation occurs through miRNA-guided transcript cleavage in plants and deadenylation followed by mRNA decay in animals (Fabian et al., 2010). Translation inhibition by miRNAs is poorly understood in plants and may entail multiple mechanisms in animals (Fabian et al., 2010; Fukaya and Tomari, 2012).

For animal miRNAs, the degrees of contribution by the two modes of action to target gene regulation have been controversial (Fabian et al., 2010). Recent studies that examined the translation inhibition and mRNA decay activities of zebrafish and *Drosophila* miRNAs with temporal resolution concluded that translation inhibition precedes target mRNA decay (Bazzini et al., 2012; Djuranovic et al., 2012). Therefore, translation inhibition is an integral and critical activity of animal miRNAs.

Unlike animal miRNAs, plant miRNAs display a high degree of sequence complementarity to their target mRNAs and were first found to guide target RNA cleavage through the endonucleolytic activity of ARGONAUTE1 (AGO1), the major miRNA effector (Baumberger and Baulcombe, 2005; Llave et al., 2002; Tang et al., 2003). This led to the assumption that RNA cleavage is the major mode of action of plant miRNAs (Jones-Rhoades et al., 2006). However, in cases in which protein accumulation from miRNA target genes was examined, plant miRNAs were found to exert disproportionate effects on target gene expression at protein versus mRNA levels (Aukerman and Sakai, 2003; Chen, 2004; Gandikota et al., 2007). Furthermore, mutations in a number of genes, including *AGO1* and *AGO10* and the P body component *VARICOSE* (*VCS*), compromise miRNA-mediated target repression at the protein, but not the mRNA, level (Brodersen et al., 2008; Yang et al., 2012). In addition, miRNAs and AGO1 are associated with polysomes (Lanet et al., 2009). These observations are usually interpreted to indicate that plant miRNAs inhibit target mRNA translation, but direct evidence showing that plant miRNAs inhibit protein synthesis from their target genes is lacking. In this study, through measurements of protein synthesis, we demonstrate that a plant miRNA indeed represses its target gene through translation inhibition.

Despite the widespread effects of plant miRNAs on target mRNA translation, the underlying mechanisms are completely unknown. Furthermore, the subcellular location where miRNA-mediated translation inhibition occurs has not been defined in eukaryotes. Here, we report that *ALTERED MERISTEM PROGRAM1* (*AMP1*), a gene that impacts multiple developmental processes in *Arabidopsis* via an unknown mechanism (Chaudhury et al., 1993; Conway and Poethig, 1997; Helliwell et al., 2001; Hou et al., 1993; Jurgens et al., 1991; Mordhorst et al., 1998), and its paralog *LIKE AMP1* (*LAMP1*) mediate the translation inhibition, but not the RNA cleavage activity, of plant miRNAs. Measurement of protein synthesis in vivo and examination of polysome profiles demonstrate that plant miRNAs inhibit target mRNA translation in an *AMP1*-dependent manner and that *AMP1* does not impact protein synthesis in general. AMP1 is an integral membrane protein associated with the rough ER, and AGO1 is a peripheral membrane protein that colocalizes with ER. We show that miRNA target transcripts are associated with microsomes but are prevented from being recruited to membrane-bound polysomes by *AMP1*. This, together with the large differences in the effects of the *amp1* mutation on the loading of miRNA target transcripts onto total versus membrane-bound polysomes, suggests that translation inhibition by plant miRNAs occurs on the ER. The presence of *AMP1* homologs in animals implies that ER may be a common site of miRNA-mediated translation inhibition in eukaryotes.

RESULTS

Mutations in *AMP1* Lead to Pleiotropic Developmental Defects

This study began with the isolation of the *amp1-30* allele in the gene *ALTERED MERISTEM PROGRAM1* (*AMP1*) (see below) from an ethyl methanesulfonate mutagenesis screen. The genetic screen was conducted in a line in which a luciferase reporter gene undergoes transcriptional gene silencing through DNA methylation (Won et al., 2012) and was designed to identify players in DNA methylation. The line also contained a mutation in *RNA DEPENDENT RNA POLYMERASE6* (*RDR6*) to prevent posttranscriptional transgene silencing (Dalmay et al., 2000; Mourrain et al., 2000). Therefore, the isolated mutant was actually a double mutant, which we refer to as *rdr6-11 amp1-30* (or *rdr6 amp1* for simplicity). *rdr6 amp1* did not show altered reporter gene expression, but its morphological phenotypes were reminiscent of those of mutants defective in miRNA biogenesis or activity and prompted us to study this mutant. Though the morphology of *rdr6* plants is largely similar to wild-type, pin-shaped cotyledons were present in 28% of *rdr6 amp1* plants (Figures 1A and 1B and Table S1). The *amp1* single mutant was later recovered and found to also exhibit radialized cotyledons (Table S1).

Defects in adaxial-abaxial polarity specification are known to result in radialized lateral organs (McConnell et al., 2001). The type III HD-Zip genes *PHABULOSA* (*PHB*), *PHAVOLUTA* (*PHV*), and *REVOLUTA* (*REV*), which are repressed by miR165/166 in the abaxial domain of organ primordia, specify adaxial identity, and failure to repress the genes leads to adaxialization and radialization of leaves (Emery et al., 2003; Mallory et al., 2004b). We thought that the phenotypes of *amp1* could reflect defects in miR165/166-mediated repression of the HD-Zip genes. To test this genetically, we crossed *amp1* with *phb-1d*/+, which harbors a miR165/166-resistant *phb* allele and displays mild leaf polarity defects (the phenotypes are mild because other HD-Zip genes are repressed by miR165/166) (McConnell et al., 2001) (Figure 1C). The *amp1 phb-1d*/+ plants had dramatic defects in leaf polarity—nearly all leaves became trumpet shaped (Figure 1D). Therefore, *amp1* is partially compromised in leaf polarity specification, and further studies revealed a defect in miR165/166-mediated repression of *PHB*, *PHV*, and *REV* (see below).

The *amp1* mutant exhibited phenotypic similarities with mutants defective in miRNA biogenesis or function. Null mutants in the miRNA biogenesis gene *DICERLIKE1* (*DCL1*) (Park et al., 2002; Reinhart et al., 2002) show overproliferation of suspensor cells (Schwartz et al., 1994). The *rdr6 amp1* mutant also showed such phenotypes (Figures 1E and 1F). Mutants in the P body gene *VCS*, which is required for miRNA-mediated translation inhibition (Brodersen et al., 2008), exhibit pointed cotyledons with incomplete veins and anthocyanin accumulation (Goeres et al., 2007). Both *rdr6 amp1* and *amp1* had incomplete veins (Figures 1G and 1H) and anthocyanin deposition in cotyledons (Figure 1B), although the phenotype was not fully penetrant (Table S1 available online). *rdr6 amp1* and *amp1* plants were also reduced in fertility (Figures 1I and 1J) and stature (Figure 1K). These phenotypes raised the possibility of *amp1* being compromised in miRNA biogenesis or activity.

AMP1 Is Required for miRNA-Mediated Target Gene Repression at the Protein, but Not at the mRNA, Level

To first evaluate whether *AMP1* plays a role in miRNA biogenesis, we performed northern blotting to compare the steady-state levels of nine miRNAs between *rdr6* and *rdr6 amp1* (Figure S1A). No difference in miRNA accumulation was observed, which argued against a role of *AMP1* in miRNA biogenesis.

Next, we examined the transcript levels of eight genes targeted by five different miRNAs using real-time RT-PCR in *rdr6 amp1* and *rdr6*. Only *CUC2* showed an increase in transcript abundance in *rdr6 amp1* relative to *rdr6* (Figure 2A). This argued against a general role of *AMP1* in miRNA-guided transcript cleavage.

Finally, we determined whether the *amp1* mutant was defective in miRNA-mediated target gene repression at the protein level. We first examined whether miR398-mediated repression of *CSD2* (Sunkar et al., 2006) was compromised in *rdr6 amp1*. miR398 is strictly induced under Cu^{2+}-limiting conditions and is not detectable under Cu^{2+}-replete conditions (Sunkar et al., 2006). We found that CSD2 protein levels were higher in *rdr6 amp1* than *rdr6* when seedlings were grown in the absence of Cu^{2+} (Figures 2B, S2A, and S2B), but *CSD2* mRNA levels were similar in the two genotypes (Figure 2A). In the presence of Cu^{2+}, CSD2 protein levels were similar in the two genotypes (Figures 2B, S2A, and S2B). This, in conjunction with the unaltered levels of miR398 (Figure S1A), suggested that miR398's activity to repress *CSD2* at the protein level was compromised in *rdr6 amp1*. The *amp1* mutation was responsible for this molecular

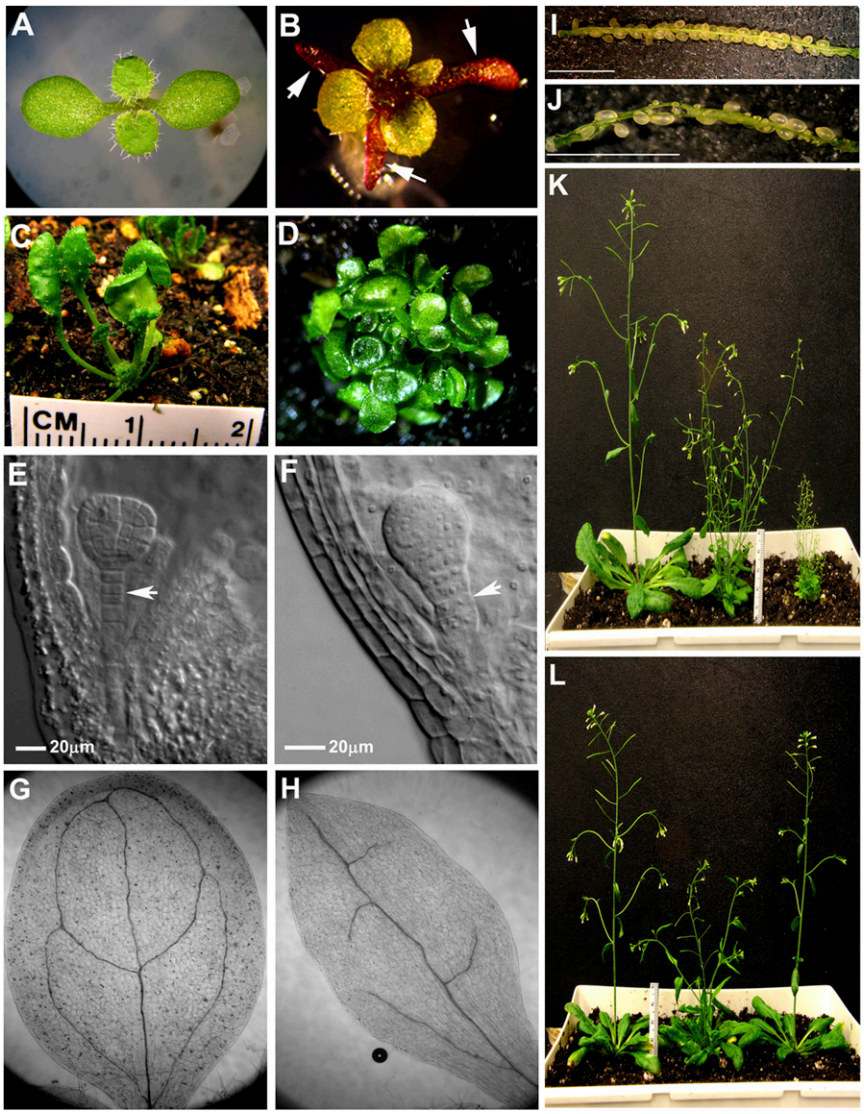

Figure 1. The *amp1-30* Mutant Exhibits Pleiotropic Developmental Defects

(A) A 12-day-old *rdr6-11* seedling with two cotyledons and two true leaves.

(B) A 12-day-old *rdr6-11 amp1-30* seedling with three pin-shaped cotyledons (marked by arrows) and four true leaves. Abnormal anthocyanin accumulation gives the seedling a purple color.

(C) A *phb-1d*/+ plant.

(D) A *phb-1d*/+ *amp1-30* plant with trumpet-shaped leaves.

(E) An *rdr6-11* embryo with a normal suspensor (arrow).

(F) An *rdr6-11 amp1-30* embryo showing over-proliferation of the suspensor (arrow).

(G) A cleared *rdr6-11* cotyledon showing venation patterns similar to those in wild-type.

(H) A cleared *rdr6-11 amp1-30* cotyledon showing incomplete venation.

(I) A dissected *rdr6-11* silique showing a full complement of seeds.

(J) A dissected *rdr6-11 amp1-30* silique with few seeds.

(I–J) Scale bars, 3 mm.

(K) Five-week-old wild-type (left), *amp1-30* (middle), and *amp1-30 lamp1-1* (right) plants.

(L) The *AMP1* gene rescues the developmental defects of the *amp1-30* mutant. (Left) Wild-type; (middle) *amp1-30*; (right) *amp1-30 AMP1p::AMP1-GFP*.

See also Table S1 and Figure S1.

defect, as the defect was rescued by *AMP1p::AMP1-HA* (Figures 2C and S2A).

To conclusively demonstrate that the increase in CSD2 protein levels in *rdr6 amp1* under Cu^{2+}-limiting conditions reflected compromised miR398 activity, we generated *CSD2p::CSD2-HA* and *CSD2p::CSD2m-HA* transgenic lines in order to compare transgene expression between *rdr6* and *rdr6 amp1*. In these lines, HA-tagged wild-type or miR398-resistant *CSD2* was driven by the *CSD2* promoter. Because plant transformation results in random transgene integration and transgene expression can be strongly influenced by transgene location, comparison of expression levels of independent transgenes in *rdr6* versus *rdr6 amp1* would not be meaningful. We obtained isogenic *rdr6* and *rdr6 amp1* lines in which each transgene was homozygous and inserted into a single genomic locus (see Extended Experimental Procedures) to enable the comparison of transgene expression between the two genotypes. We found that, under Cu^{2+}-limiting conditions (i.e., miR398 present), CSD2-HA levels were higher in *rdr6 amp1* than *rdr6*, but CSD2m-HA levels were similar in the two genotypes (Figures 2D and S2C). This demonstrated that miR398-mediated repression of *CSD2* at the protein level was compromised by the *amp1* mutation.

We next determined whether *AMP1* also mediates the activities of other miRNAs. We generated isogenic *rdr6* and *rdr6 amp1* lines containing each of the following transgenes: *35S::PHB-MYC*, *35S::CNA- MYC*, and *35S::REV- MYC* (all targeted by miR165/6 [Rhoades et al., 2002; Tang et al., 2003]), and *35S::CUC1- MYC* (targeted by miR164 [Mallory et al., 2004a]). Note that the inclusion of the *rdr6* mutation in these analyses was necessary to prevent transgene silencing. For each transgene, at least two independent transgenic events were evaluated. In all cases, an increase in transgene protein levels was found in *rdr6 amp1* relative to *rdr6* (Figures 2E, 2F, S2D, S2E, S2F, and S2G). The miR165/6-resistant *35S::PHBm-MYC* transgene was similarly expressed in *rdr6 amp1* and *rdr6* (Figures 2E and S2D). The transcript levels from each of the transgenes were similar in *rdr6* and *rdr6 amp1* except for *CUC1-MYC* (Figure 2G).

To rule out an effect of *amp1* on miRNA-mediated transcript cleavage, we performed semiquantitative 5′ RACE RT-PCR to detect the 3′ cleavage products from five miRNA target genes in *rdr6* and *rdr6 amp1*. No difference in the abundance of the

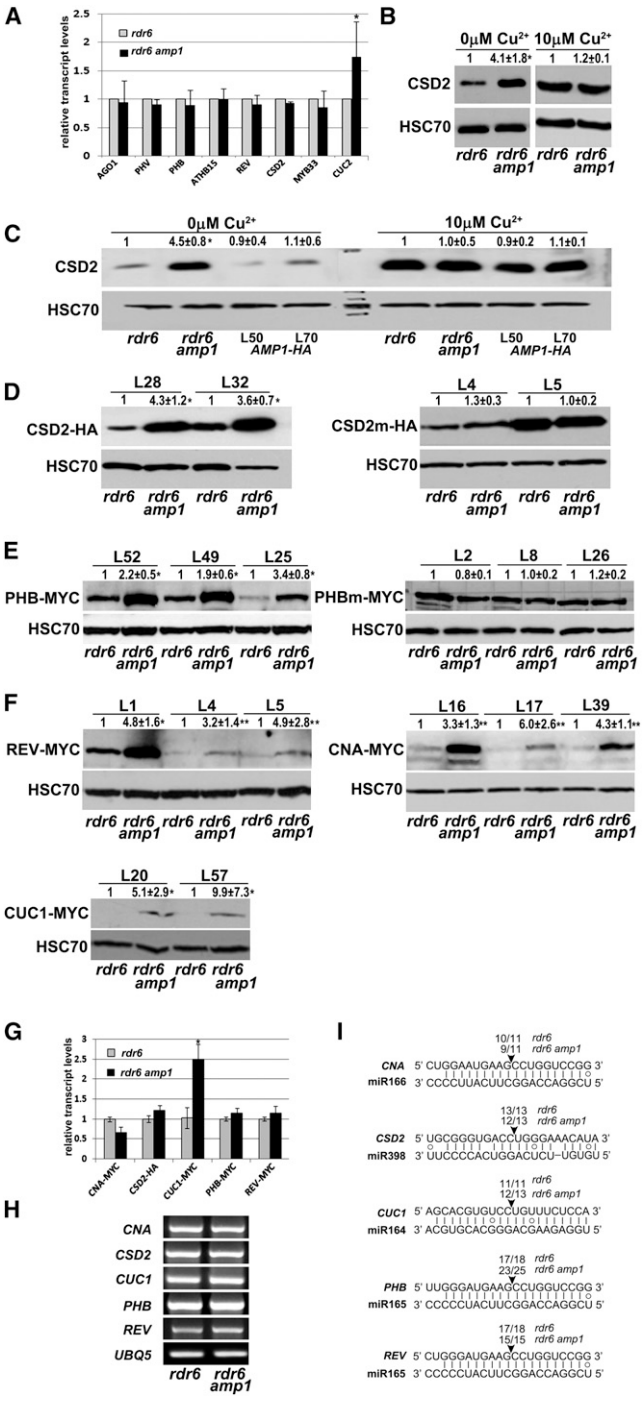

Figure 2. *AMP1* Is Dispensable for miRNA-Mediated Transcript Cleavage but Is Required for the Activities of miRNAs in Repressing the Protein Levels of Target Genes

(A) Steady-state levels of transcripts from eight miRNA target genes as determined by real-time RT-PCR. *UBQ5* was used as an internal control. Error bars represent SD calculated from three independent experiments.

(B–F) Western blots to determine the levels of various proteins. HSC70 served as the loading control. One biological replicated is shown; two others are in Figure S2. The numbers above the blots indicate relative protein levels as calculated from the three biological replicates.

(B and C) CSD2 protein levels in various genotypes under Cu^{2+}-limiting (miR398 present) and Cu^{2+}-replete (miR398 absent) conditions. L50 and L70 are two independent *AMP1p::AMP1-HA* transgenic lines in the *rdr6 amp1* background.

(D) Levels of CSD2-HA or CSD2m-HA from *rdr6* and *rdr6 amp1* plants carrying a homozygous transgene at the same genomic location. L28 and L32 are two independent transgenic events for *CSD2p::CSD2-HA*; L4 and L5 are two independent transgenic events for *CSD2p::CSD2m-HA*. Plants were grown under Cu^{2+}-limiting conditions.

(E) Levels of PHB-MYC or PHBm-MYC from *rdr6* and *rdr6 amp1* plants carrying a homozygous transgene at the same genomic location. L52, L49, and L25 are three independent transgene insertion events for *35S::PHB-MYC*; L2, L8, and L26 are three independent transgene insertion events for *35S::PHBm-MYC*.

(F) Levels of REV-MYC, CNA-MYC, and CUC1-MYC proteins. For each transgene, two to three independent transgene insertion events (as indicated by L followed by a number above the gel images) were evaluated.

(G) Real-time RT-PCR to examine transcript levels from various transgenes in (D–F). Values were normalized to *UBQ5*. Error bars represent SD calculated from three independent experiments.

(H) Semiquantitative 5′ RACE-PCR to detect the 3′ fragments generated through miRNA-guided cleavage of various target transcripts. *UBQ5* is a loading control.

(I) Mapping the position of miRNA-guided cleavage by cloning and sequencing the 5′ RACE products in (H). The miRNAs that target the transcripts are shown. The numbers above the sequences indicate the number of clones representing cleavage at the expected position (arrowhead) out of the total number of clones sequenced.

*$p < 0.05$; **$p < 0.01$. See also Figure S2.

3′ cleavage products was detected (Figure 2H). In addition, the cleavage products were cloned and sequenced, which revealed that the precision of miRNA-mediated RNA cleavage was unaffected by the *amp1* mutation (Figure 2I).

In conclusion, *AMP1* is not required for miRNA-mediated cleavage of target mRNAs; instead, it mediates the activities of multiple miRNAs in reducing the protein levels of their target genes. The lack of an effect of the *amp1* mutation on protein accumulation from miRNA-resistant transgenes indicates that *AMP1* does not affect protein levels in general.

A Plant miRNA Inhibits the Translation of Its Target mRNA in an *AMP1*-Dependent Manner

Although the disproportionate effects of plant miRNAs on target gene expression at protein versus mRNA levels have been attributed to their translation inhibition activities, plant miRNAs have not been definitively shown to inhibit protein synthesis. We took advantage of the *amp1* mutant to determine whether plant miRNAs inhibit protein synthesis from their target mRNAs. To this end, we first determined the half-life of the CSD2-HA protein from a *CSD2p::CSD2-HA* transgenic line through pulse-chase experiments. We found the half-life to be at least 12 hr under Cu^{2+}-limiting conditions (data not shown). The long half-life allowed us to ascertain protein synthesis rates from the transgene by incubating seedlings in ^{35}S-Methionine media for short time periods (20 min and 40 min) followed by immunoprecipitation of CSD2-HA. The immunoprecipitated and radiolabeled CSD2-HA represented newly synthesized CSD2-HA, whereas western blots on the same samples displayed the steady-state levels of the protein (both labeled and unlabeled). As expected, in both *rdr6* and *rdr6 amp1*, the amount of radiolabeled CSD2-HA increased over time, but the steady-state levels were the same at the two time points (Figures 3A, 3B, and S3A). The

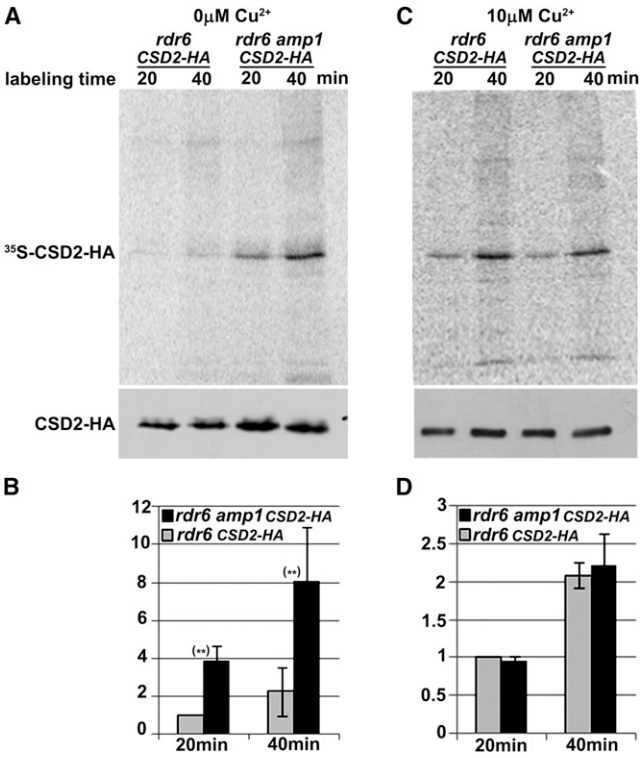

Figure 3. Measurement of Protein Synthesis from a *CSD2p::CSD2-HA* Transgene in the *rdr6* or *rdr6 amp1* Background

(A and C) Isogenic *rdr6 CSD2p::CSD2-HA* and *rdr6 amp1 CSD2p::CSD2-HA* seedlings (L32 in Figure 2D) were labeled with ^{35}S-Methionine for 20 or 40 min under Cu^{2+}-limiting (miR398 present) or Cu^{2+}-replete (miR398 absent) conditions. CSD2-HA was then immunoprecipitated, resolved by SDS-PAGE, and transferred to a membrane. The membrane was first subjected to western blotting to detect steady-state levels of CSD2-HA (bottom gel images) and then to autoradiography to detect labeled CSD2-HA (^{35}S-CSD2-HA). Note that the steady-state CSD2-HA levels serve as a loading control. Under Cu^{2+}-limiting conditions, the difference in steady-state CSD2-HA levels between *rdr6* and *rdr6 amp1* was already known (Figure 2D). By referencing Figure 2D, we conclude that the loading was comparable for *rdr6* and *rdr6 amp1*. Under Cu^{2+}-replete conditions, CSD2-HA steady-state levels should be nearly equal (Figure 2C). Therefore, loading was even for the four samples.

(B and D) Quantification of ^{35}S-CSD2-HA signals in (A) and (C). The *rdr6* 20 min sample was arbitrarily set to 1.0.

The quantification was based on three independent replicates, and error bars represent SD. $^{**}p < 0.01$. See also Figure S3.

amount of newly synthesized CSD2-HA was higher at both time points in *rdr6 amp1* than *rdr6* under Cu^{2+}-limiting conditions (Figures 3A, 3B, and S3A). Therefore, *AMP1* was required for the inhibition of protein synthesis from *CSD2-HA*. To determine whether the translation inhibition by *AMP1* required miR398, we performed the pulse-labeling experiments in the presence of Cu^{2+}. The amount of newly synthesized CSD2-HA was similar in *rdr6* and *rdr6 amp1* under Cu^{2+}-replete conditions (Figures 3C, 3D, and S3B). Therefore, miR398 inhibits protein synthesis from the *CSD2p::CSD2-HA* transgene in an *AMP1*-dependent manner. Furthermore, the general profiles of labeled proteins were identical in *rdr6* and *rdr6 amp1* (Figure S3C), indicating that *AMP1* does not impact protein synthesis in general.

AMP1 Belongs to a Conserved Protein Family in Eukaryotes

Using a map-based cloning strategy, we identified the molecular lesion of *amp1-30* as a G-to-A change in the splice junction at the sixth intron in the *AMP1* gene (Figure 4A). Two genomic clones, *AMP1p::AMP1-GFP* and *AMP1p::AMP1-HA*, both fully rescued the morphological defects (Figure 1L) as well as the molecular defects of *rdr6 amp1* (i.e., the increase in CSD2 protein levels; Figures 2C and S2A), demonstrating that *AMP1* mediates the activities of miRNAs.

Homologs of plant *AMP1* are easily recognized in animals (Figure 4A). These included six human genes—four encoding confirmed or putative glutamate carboxypeptidases or N-acetylated α-linked acidic dipeptidases (NAALADase) and two encoding the transferrin receptor. AMP1 and its homologs share a common organization of motifs/domains: an N-terminal transmembrane domain, a protease-associated (PA) domain, a peptidase domain, and a transferrin receptor dimerization domain (Figure 4A).

The presence of the peptidase domain in AMP1 raised the possibility that AMP1 acts to degrade proteins from miRNA target genes. Although this scenario would be consistent with AMP1's role in repressing miRNA target gene expression at the protein level, it is not likely, as we had shown that AMP1 inhibits protein synthesis (i.e., translation) from miRNA target genes (Figure 3). Nonetheless, we examined whether AMP1 affects the half-life of miRNA target proteins by performing pulse-chase experiments. As the long half-life of CSD2-HA made it unsuitable for this analysis, we focused on PHB-MYC with a much shorter half-life. The half-lives of PHB-MYC in *rdr6 PHB-MYC* and *rdr6 amp1 PHB-MYC* were not significantly different as measured from three independent experiments (Figures S3D and S3E), thus ruling out a role of AMP1 in degrading PHB-MYC.

An *AMP1* paralog (At5g19740), *LAMP1*, encoding a protein with 42% amino acid similarity to AMP1 is present in the *Arabidopsis* genome (Figure 4A). We identified a T-DNA insertion mutant, *lamp1-1*, and produced the *amp1-30 lamp1-1* double mutant (in the wild-type *RDR6* background; will be referred to as *amp1 lamp1*). The double mutant was extremely small (Figures 1K and 4B) and sterile (Figure 4C), suggesting that the two genes have overlapping functions in development. The two genes also have overlapping molecular functions. miR398-mediated repression of *CSD2* was more compromised in *amp1 lamp1* than in *amp1* (Figures 4D and S2H). The *amp1 lamp1* double mutant, but not the *amp1* single mutant, showed an increase in the protein, but not the transcript, levels from the *AGO1* gene, which is targeted by miR168 (Vaucheret et al., 2004) (Figures 4E, 4F, and S2I). The *amp1 lamp1* double mutant had normal levels of various miRNAs (Figure S1B), as well as most miRNA target mRNAs (Figure 4F), suggesting that both genes mediate the translation inhibition activities of miRNAs. Note that a significant increase in CSD2 protein levels was observed in *rdr6 amp1* relative to *rdr6* (Figure 2D) but not in *amp1* relative to WT (Figure 4D). This suggests that the *rdr6* mutation somehow enhances *amp1*'s defects in miRNA-mediated translation repression. We suspect that this reflects an indirect effect of *RDR6*, which enables the production of endogenous siRNAs (Peragine et al., 2004; Vazquez et al., 2004) that may share with miRNAs the translation repression

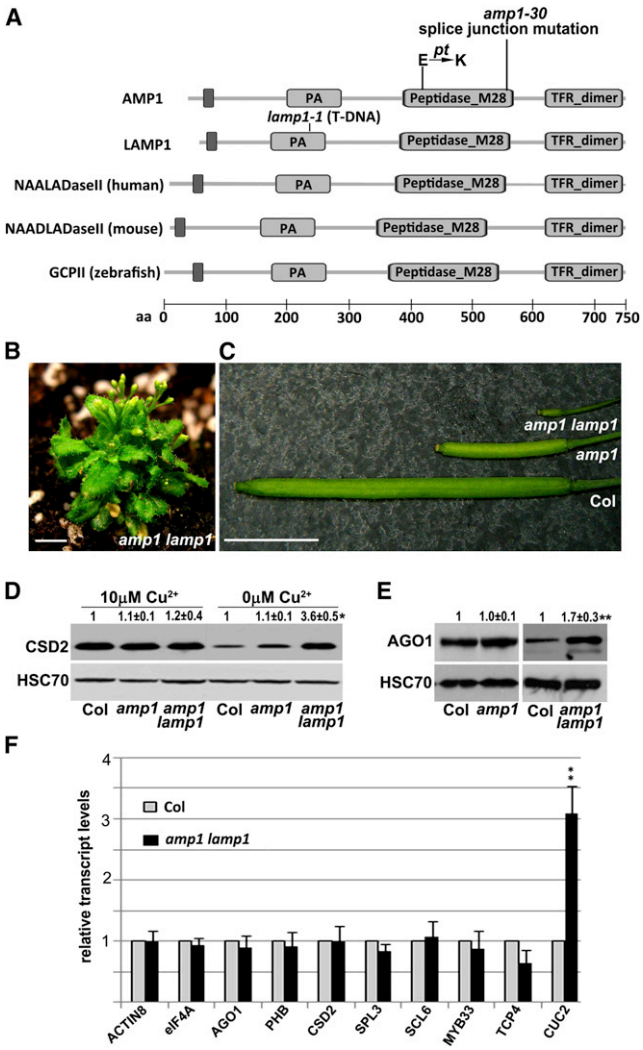

Figure 4. *AMP1* and Its Paralog *LAMP1* Have Overlapping Functions in Mediating the Translation Inhibition Activities of miRNAs

(A) Diagrams of AMP1, LAMP1, and three animal AMP1 homologs. The molecular lesions in two *amp1* alleles are shown. PA, protease-associated domain; Peptidase_M28, a Pfam peptidase domain; TFR_dimer, a dimerization domain in transferrin receptor. *pt* is a previously described *amp1* allele (Helliwell et al., 2001).

(B) The *amp1 lamp1* double mutant is extremely dwarfed. Scale bar, 6 mm.

(C) Siliques from wild-type (Col), *amp1*, and the *amp1 lamp1* double mutant. Scale bar, 6 mm.

(D and E) Western blots to determine CSD2 (D) and AGO1 (E) protein levels in wild-type (Col), *amp1*, and *amp1 lamp1*. Note that the two AGO1 panels cannot be compared with each other due to differences in exposure time. Protein levels (mean ± SD) were calculated from three biological replicates.

(F) Real-time RT-PCR to determine the transcript levels of eight miRNA target genes and two nontargets (*ACTIN8* and *eIF4A*) in wild-type (Col) and *amp1 lamp1*. Values were normalized to *UBQ5*. Error bars represent SD calculated from three independent experiments.

(D–F) *$p < 0.05$; **$p < 0.01$.

machinery involving *AMP1*. The absence of endogenous siRNAs in *rdr6* may allow miRNAs better access to the machinery to exert a stronger effect in translation repression.

AMP1 and AGO1 Are Localized to the ER

Given that both AMP1 and the miRNA effector AGO1 are required for miRNA-mediated translation repression (this study and Brodersen et al., 2008), we sought to determine whether the two proteins are associated or colocalize in vivo. Immunoprecipitation (IP) was conducted using anti-GFP antibodies with extracts from *rdr6* and *AMP1p::AMP1-GFP rdr6 amp1* plants. Western blotting using anti-AGO1 antibodies showed that AGO1 was enriched in the IP (Figure 5A). In the reciprocal experiment, in which AGO1 was immunoprecipitated from *rdr6* and *AMP1p::AMP1-HA rdr6 amp1* plants, AMP1-HA was found enriched in the IP (Figure 5B). This suggested that the two proteins are associated in vivo.

A previous study showed that GFP-AMP1 from a *35S::GFP-AMP1* transgenic line localized to the endoplasmic reticulum (ER) in *Arabidopsis* (Vidaurre et al., 2007), consistent with the presence of a transmembrane domain in AMP1. We sought to confirm the ER localization of AMP1 and determine whether AGO1 is also associated with ER. When transiently expressed in *Nicotiana benthamiana*, AMP1-GFP and ER-mCherry, an ER marker (Nelson et al., 2007), were found to colocalize in mesh-like patterns typical for the ER (Figures 5C–5E). In leaves coexpressing YFP-AGO1 and ER-mCherry, YFP-AGO1 accumulated in many cytoplasmic granules that colocalized with ER-mCherry (Figures 5F–5H, S4A, and S4B). Quantification of YFP-AGO1 signals revealed that most AGO1 granules were along the ER meshwork (Figure 5I). DECAPPING1 (DCP1), a P body marker, was also found in cytoplasmic granules (Movie S3) (Xu et al., 2006), but the DCP1 foci did not colocalize with ER-mCherry (Figure 5I and Movie S3).

To examine the membrane association of AMP1 and AGO1 in *Arabidopsis*, we separated extracts from an *AMP1p::AMP1-HA rdr6 amp1* line into crude membrane and soluble fractions. AMP1-HA was exclusively in the membrane fraction (Figure 5J), and AGO1 was enriched in the membrane fraction (Brodersen et al., 2012) (Figure 5J). Under high-salt or high-pH conditions, AGO1 was displaced into the soluble fraction (Brodersen et al., 2012) (Figure 5K), whereas AMP1-HA remained in the membrane fraction (Figure 5K). Therefore, AMP1 is an integral membrane protein, whereas AGO1 is a peripheral membrane protein. We further examined whether the membrane association of AGO1 was dependent on AMP1. Similar fractionation studies were conducted with *rdr6* and *rdr6 amp1*. No difference in the distribution of AGO1 between soluble and membrane fractions was found in the two genotypes (Figure S4A), indicating that AMP1 is not required for the membrane association of AGO1.

Sucrose-gradient-based membrane fractionation with a *35S::GFP-AMP1* line showed a shift of GFP-AMP1 to lighter fractions upon ribosome dissociation in the absence of Mg^{2+} (Vidaurre et al., 2007), suggesting that AMP1 is present on the rough ER. To confirm this finding with an *AMP1* transgene driven by its own promoter, we fractionated membranes with the *AMP1::AMP1-GFP rdr6 amp1* line and examined the distribution of AMP1-GFP and AGO1 along the sucrose gradient. In the presence of Mg^{2+}, AMP1-GFP was found in dense and medium-dense fractions, and AGO1 was in medium dense fractions (Figure S4B). In the presence of EDTA that chelates

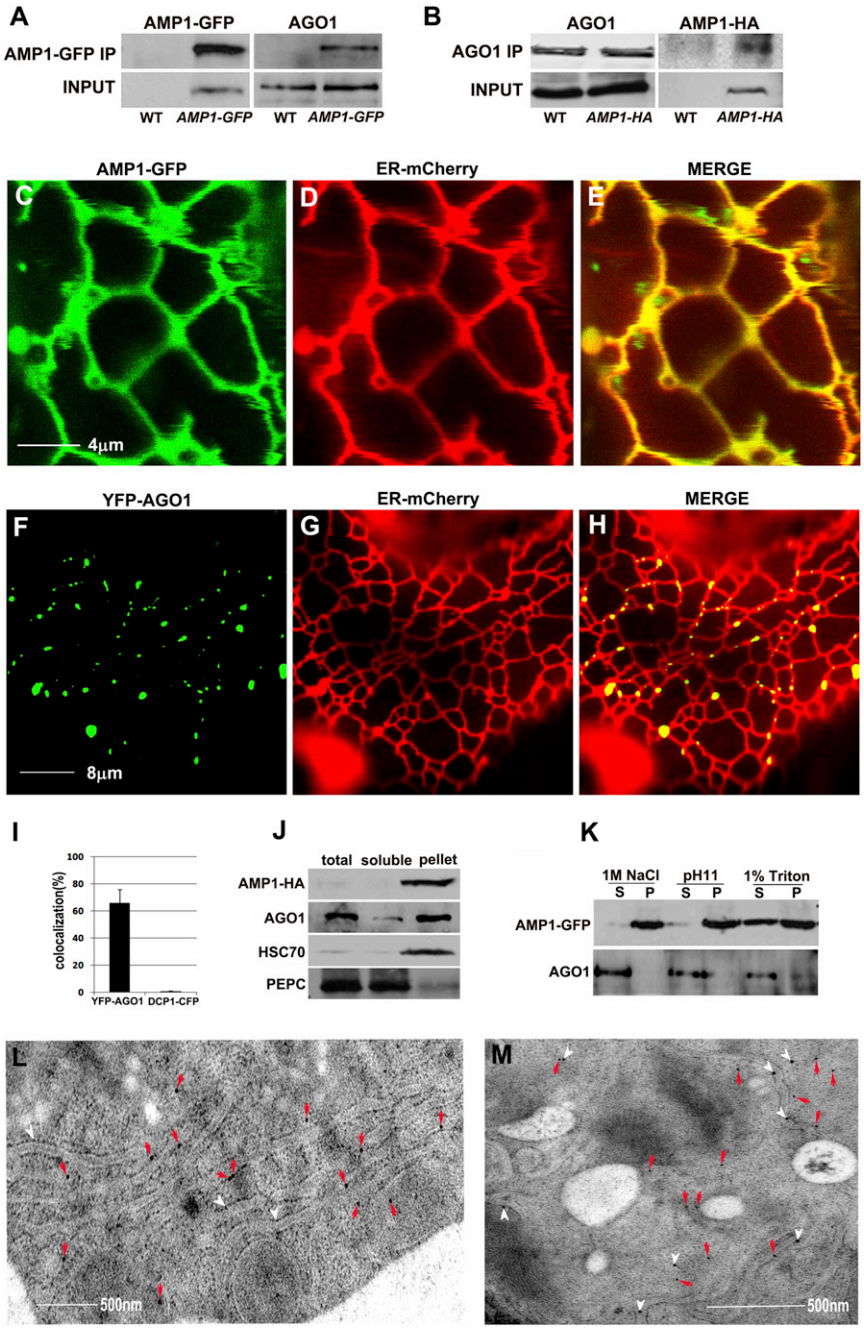

Figure 5. AMP1 and AGO1 Are Associated In Vivo, and Both Are Localized to the ER

(A) Co-IP performed with an *AMP1p::AMP1-GFP rdr6 amp1* line, in which the transgene fully rescues the *amp1* phenotypes. WT, *rdr6* plants without the transgene. IP was performed with anti-GFP antibodies, and the immunoprecipitates were subjected to western blotting with anti-GFP (left) or anti-AGO1 (right) antibodies.

(B) Co-IP performed with an *AMP1p::AMP1-HA rdr6 amp1* line, in which the transgene fully rescues the *amp1* phenotypes. WT, *rdr6* plants without the transgene. IP was conducted with anti-AGO1 antibodies, and the immunoprecipitates were subjected to western blotting with anti-AGO1 (left) or anti-HA (right) antibodies. 1% of lysate was used to extract proteins as input in (A) and (B).

(C–H) Colocalization of AMP1-GFP or YFP-AGO1 with ER-mCherry. AMP1-GFP (C–E) or YFP-AGO1 (F–H) was transiently coexpressed with ER-mCherry in *N. benthamiana* leaves. Fluorescence was observed separately (C and D; F and G), and the images were merged (E, H).

(I) Quantification of colocalization between YFP-AGO1 or DCP1-CFP and ER-mCherry. Confocal z stacks were collected from 30 and 23 cells for YFP-AGO1 and DCP1-CFP, respectively, and colocalization was quantified with the image analysis software IMARIS7.2. Values are expressed as mean ± SD.

(J) AMP1-HA and AGO1 are present in a crude membrane fraction. Western blots were performed to detect various proteins in the total extract, the soluble fraction, or the pellet after centrifugation at 100,000 × *g*. PEPC and HSC70 are a cytosolic and an ER lumenal protein, respectively.

(K) AMP1 is an integral membrane protein, whereas AGO1 is a peripheral membrane protein. Western blots were performed to detect the presence of AMP1-GFP and AGO1 in the soluble fraction (S) or the pellet (P) after membrane suspensions in buffers containing high-salt or detergent concentrations or high pH were centrifuged at 100,000 × *g*. *AMP1p::AMP1-GFP rdr6 amp1* plants were used for the assays.

(L) A TEM image of a root tip section from an *AMP1p::AMP1-HA rdr6 amp1* line immunolabeled with anti-HA antibodies. All immunogold particles are marked by red arrows. White arrowheads indicate ribosome particles on the surface of ER. Most ER tubules in the images are dotted with ribosomes and hence are rough ER.

(M) A TEM image of a root tip section from an *AMP1p::AMP1-HA rdr6 amp1* line immunolabeled for AMP1-HA (15 nm gold particles; white arrows) and Calnexin (10 nm gold particles; red arrows).

See also Table S2 and Figure S4.

Mg^{2+}, AMP1-GFP shifted to medium-dense and light fractions, and AGO1 shifted to light fractions (Figure S4B). The Mg^{2+}-induced shift toward heavier fractions for the two proteins suggests that both are associated with membranes bound by ribosomes or large protein complexes. The distribution of the two proteins in the presence of Mg^{2+} partially overlapped, consistent with the two proteins acting together.

To confirm the rough ER localization of AMP1, we performed immunogold labeling for AMP1-HA in an *AMP1p::AMP1-HA rdr6 amp1* line and wild-type (a negative control). AMP1-HA signals in *AMP1p::AMP1-HA rdr6 amp1* were associated with tubular structures characteristic of ER (Figure 5L). Quantification of AMP1-HA signals in *AMP1p::AMP1-HA rdr6 amp1* and wild-type revealed that the labeling was specific (Table S2).

Colocalization with the ER marker Calnexin confirmed the ER localization of AMP1-HA (Figure 5M). The ER with AMP1-HA signals was also associated with ribosomes (Figure 5L), suggesting that AMP1 localizes to the rough ER. However, as rough ER was the main form of ER in the root tip cells examined, we could not exclude an association of AMP1 with smooth ER.

In conclusion, AMP1 is an integral membrane protein localized on the rough ER. AGO1 is a peripheral ER membrane protein that is also possibly associated with the rough ER. The rough ER association of AGO1 is supported by the observed Mg^{2+}-induced shift in sucrose gradients (Figure S4B) and the presence of AGO1 on polysomes (Lanet et al., 2009). Given the ER association of both proteins, the observed co-IP between AMP1 and AGO1 (Figures 5A and 5B) could be attributable to the two proteins being in close proximity on the same membrane rather than being in the same protein complex.

miRNA Target Transcripts Are Similarly Associated with Total Polysomes in Wild-Type and *amp1 lamp1*

To begin to determine how *AMP1* mediates the translation inhibition activity of miRNAs, we examined the distribution of miRNA target transcripts along polysomes in wild-type and the *amp1 lamp1* double mutant. We first extracted total polysomes (TPs), which are composed of soluble as well as membrane- and cytoskeleton-associated polysomes, and resolved them on sucrose density gradients. The A254 absorption profiles of TPs from WT and *amp1 lamp1* were largely similar (Figure S5A), suggesting that *AMP1* does not affect translation in general. The TP gradient was collected into 17 fractions, and the amount of mRNAs in each fraction was determined by real-time RT-PCR. Five miRNA target transcripts—*PHB*, *CSD2*, *CUC2*, *SCL6*, and *TCP4* (all targeted by different miRNAs) —as well as the nontarget *UBQ5* RNA were similarly distributed along the TP profiles in wild-type and *amp1 lamp1* (Figure S5B).

miRNA Target Transcripts Show Enhanced Association with Membrane-Bound Polysomes in *amp1 lamp1*

The requirement for ER-localized AMP1 for the translation inhibition activity of miRNAs suggests that miRNAs inhibit the translation of their target mRNAs on the ER. To test this hypothesis, we examined the distribution of miRNA target transcripts along membrane-bound polysomes (MBPs). We isolated microsomes through sucrose-step gradient centrifugation (Figure 6A) using optimized conditions that allowed for the preservation of AMP1, AGO1, and intact ribosomal RNAs in the microsomes (Figures S5C and S5D). The quality of the microsome fraction was shown by the presence of the ER membrane protein SEC12, the absence of the soluble protein PEPC, and the type and quality of the rRNA species (Figures S5C and S5D). We first quantified the levels of various transcripts, including those targeted by miRNAs, in the microsome fraction. The proportion of microsome-associated RNA in total RNA for most tested genes—both miRNA targets as well as nontargets such as *UBQ5*, *eIF4A*, and *ACTIN8*—was similar in wild-type and *amp1 lamp1* (Figure 6B), suggesting that *AMP1* is not required for the membrane association of these transcripts. AMP1 is also dispensable for the membrane association of the AGO1 protein. AGO1 was present in the microsome fraction in both wild-type and *amp1 lamp1* and was at a higher level in the latter (Figure 6C), consistent with its increased abundance in the double mutant (Figures 4E and S2I).

We next extracted membrane-bound polysomes (MBPs) from the microsome fraction and subjected the MBPs to sucrose density gradient fractionation (Figure 6A). The A254 absorption profiles of MBPs (from either wild-type or *amp1 lamp1*) differed from those of TPs in that the 80S peak was smaller (compare Figures 6D and S5A). Similar observations were made for MBPs from other organisms (Birckbichler and Pryme, 1973; Noll and Burger, 1974). The MBP gradients were collected into 17 fractions, and the amount of mRNAs in each fraction was quantified by real-time RT-PCR. miRNA target transcripts, such as *AGO1*, *PHB*, *CSD2*, *SPL3*, *SCL6*, and *TCP4*, showed a significant increase in MBP association in the double mutant, whereas nontarget transcripts such as *UBQ5*, *eIF4A*, *ACTIN8*, At2g01570, At5g28770, and At5g66770 were similarly distributed along MBP fractions in wild-type and *amp1 lamp1* (Figure 6E). Note that At2g01570, At5g28770, and At5g66770, which encode transcription factors, were included in the analysis because their transcript levels were more similar to those of the miRNA target transcripts than the abundant *UBQ5*, *eIF4A*, and *ACTIN8* transcripts. The similar degree of microsome association of miRNA target transcripts in wild-type and *amp1 lamp1* (Figure 6B) contrasts with their preferential loading onto MBPs in *amp1 lamp1* (Figure 6E) and indicates that miRNAs inhibit the translation of their target transcripts on membranes. The requirement for the ER protein AMP1 for this activity suggests that ER is the site of miRNA-mediated translation inhibition.

DISCUSSION

ER as the Site of miRNA-Mediated Translation Repression

The subcellular location where miRNAs repress the translation of their target mRNAs has been unknown. In this study, we show that miRNA-mediated translation inhibition, but not target RNA cleavage, requires *AMP1*. Characterization of the subcellular localization of AMP1 and comparison of the distribution of miRNA target RNAs on TPs versus MBPs reveal that miRNA-mediated translation inhibition occurs on the ER. Given that homologs of *AMP1* are present in animal genomes, it is possible that the connection between the ER and translation inhibition by miRNAs is conserved. Consistent with this, miRNA effectors—AGO1 in plants and Ago2 in mammals—are membrane associated (Brodersen et al., 2012; Cikaluk et al., 1999).

It is of interest to integrate the knowledge of the ER as the site of translation inhibition by miRNAs with existing knowledge on the subcellular compartmentalization of miRNA biogenesis/action. This study, together with several studies in animals (Gibbings et al., 2009, 2012; Lee et al., 2009), establishes the endomembrane system as an important site where miRNA biogenesis/action or its regulation takes place. On the other hand, cytoplasmic granules such as P bodies have also been implicated in RNA silencing (Fabian et al., 2010). Genetic evidence supports a role of the P body component *VCS* in miRNA-mediated translational

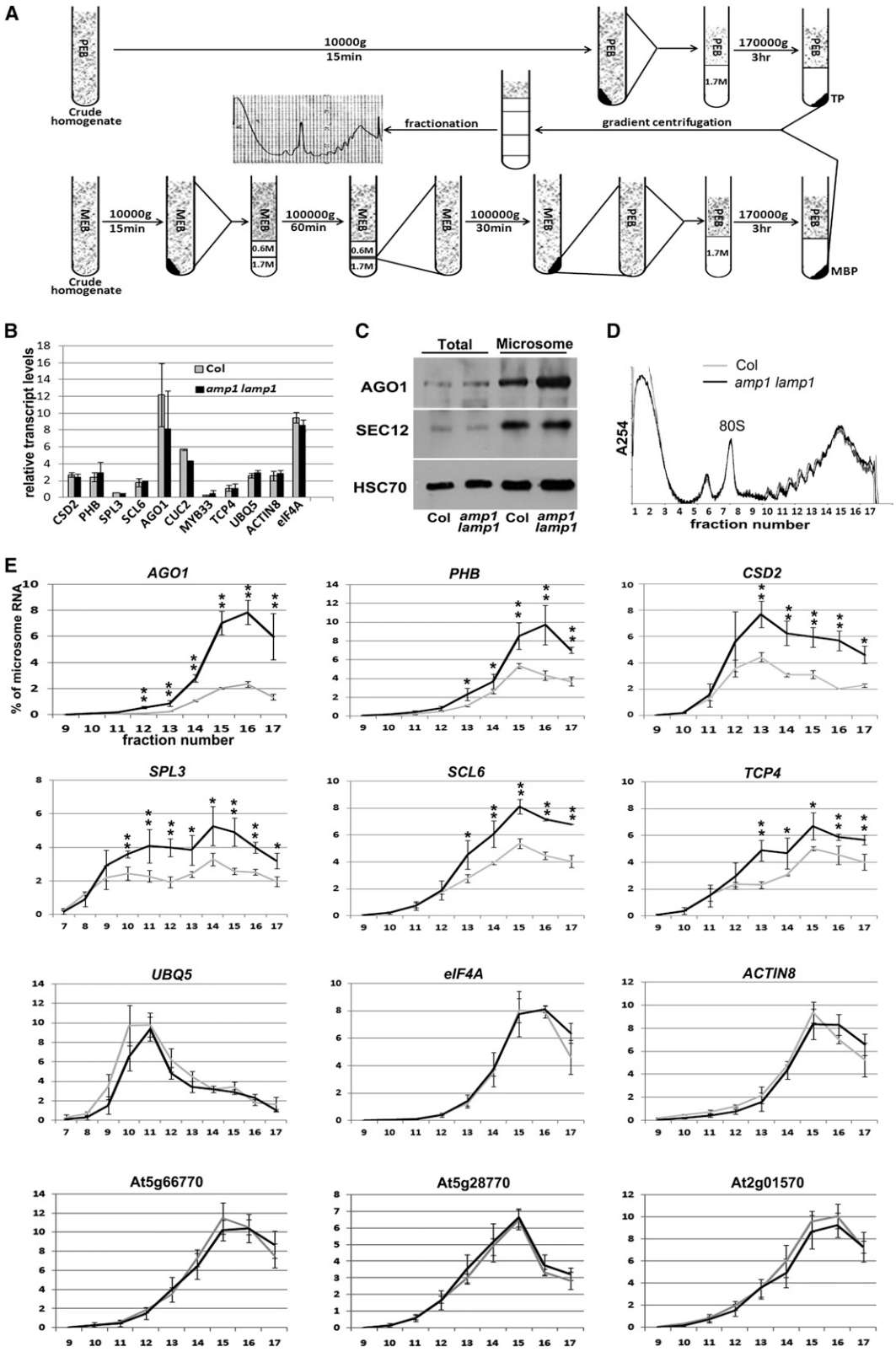

(legend on next page)

repression in *Arabidopsis* (Brodersen et al., 2008). In cultured human cells, the miRNA let-7 and its target transcript are both localized to cytoplasmic foci adjacent to P bodies (Pillai et al., 2005). How translation repression on the ER is mechanistically connected to P bodies is currently unknown. The P body component DCP1 does not colocalize with ER (Figure 5I and Movie S3).

Translation on the ER Is Not Restricted to mRNAs Encoding Membrane or Secreted Proteins

Our studies also ascribe a new function to the ER. ER is well known as the site of translation of mRNAs encoding membrane or secreted proteins. The classical view is that mRNAs encoding membrane or secreted proteins are recruited to the ER via the signal recognition particle in a translation-dependent manner. However, many studies report puzzling observations that a large portion of the yeast or mammalian transcriptome, including numerous transcripts encoding soluble proteins, is ER-associated or translated on membrane-bound polysomes (Kraut-Cohen and Gerst, 2010; Lerner et al., 2003; Reid and Nicchitta, 2012). Although the ER association of transcripts is likely to have multifaceted functions, we propose that one function is to allow miRNA-mediated inhibition of translation to occur. We envision that miRNA target transcripts are sequestered on the ER or in a compartment linked to the ER to prevent their translation. Although the prevention of their translation requires *AMP1*, the membrane association of the transcripts, as well as the AGO1 protein, occurs in an *AMP1*-independent manner.

ER-Cytosol Partitioning of Translation and miRNA Activities

The similar loading of miRNA target transcripts onto TPs and the differential loading of the transcripts onto MBPs in wild-type and *amp1 lamp1* indicate that miRNA-mediated translation inhibition occurs on membranes. Given that a small portion (less than 15%) of the total transcript pool of a miRNA target gene is associated with microsomes (Figure 6B), how could the inhibition of this portion result in the observed differences in protein output between wild-type and *amp1 lamp1*? We suspect that the observed levels of membrane-associated transcripts (Figure 6B) were an underestimate because membrane breakage during the experimental procedure would reduce the yield of intact microsomes. However, it is still likely that a large fraction of the transcript pool is present in the cytosol, and it remains an open question of whether ER-associated translation inhibition is sufficient to contribute to the overall activities of miRNAs. One possibility is that translation in the cytosol is also inhibited by miRNAs, and the lack of differences in transcript distribution along TPs between wild-type and *amp1 lamp1* could be due to pseudo-polysomes (large RNA-protein complexes) induced by miRNAs, which were observed in *Drosophila* (Thermann and Hentze, 2007). However, under this scenario, translation inhibition in the cytosol also needs to be *AMP1* dependent for it to account for the protein output differences between wild-type and *amp1 lamp1*. An alternative hypothesis is that translation on the ER is much more efficient than that in the cytosol, such that inhibition of a small, ER-associated portion of the transcript pool is sufficient to account for the differences in protein output. In fact, an analysis of ER-cytosol partitioning of transcripts and their translation status as reflected by their ribosome association in HEK293 cells suggested that ER serves as the site of translation for a broad set of transcripts, including those encoding soluble proteins (Reid and Nicchitta, 2012). Furthermore, the study suggested that translation is more efficient on the ER than in the cytosol in terms of ribosome density per transcript, as well as the processivity of translation elongation (Reid and Nicchitta, 2012).

The Translation Inhibition Activity of Plant miRNAs Is Probably Crucial for Development

Plant miRNAs are key players in almost all developmental events and regulate target transcripts through two modes of action: cleavage and translation inhibition. Previous studies on a number of miRNAs such as miR156, miR172, and miR398 show that both modes of action act upon the same target transcripts (Aukerman and Sakai, 2003; Brodersen et al., 2008; Chen et al., 2004; Chen, 2004; Gandikota et al., 2007; Kasschau et al., 2003; Schwab et al., 2005; Sunkar et al., 2006). In this study, we extend similar observations to miR164 and miR165/6 and show that the two modes of action are genetically separable (Figure 2). This raises the question regarding each mode of action's relative contribution to plant development. The cleavage activity is likely crucial for plant development, as a slicer-defective *AGO1* transgene fails to rescue the developmental defects of an *ago1* null mutant (Carbonell et al., 2012). How about the contribution of translation inhibition to plant development?

Mutations in *AMP1* lead to pleiotropic developmental defects such that *amp1* alleles were independently isolated in a number of genetic screens focusing on various aspects of plant development, and the gene was given many names, such as *AMP1* (Chaudhury et al., 1993), *CONSTITUTIVE MORPHOGENESIS2*

Figure 6. Profiles of Membrane-Bound Polysomes from Wild-Type and the *amp1 lamp1* Double Mutant, and the Distribution of Various mRNAs along MBPs

(A) A diagram showing the schemes used for the isolation of total polysomes (TPs) and MBPs.

(B) Quantification of various transcripts in the microsome fraction by real-time RT-PCR. Eight miRNA target mRNAs and three nontargets (*UBQ5*, *ACTIN8*, and *eIF4A*) were assayed. The amount of a transcript in the microsome fraction is expressed as a proportion of the total amount for the RNA in the cell. The error bars were calculated from three biological repeats.

(C) *AMP1* or *LAMP1* is not required for the microsome association of AGO1. Western blots were performed to determine the levels of AGO1 in total extract and in the microsome fraction. SEC12 and HSC70 serve as an ER marker and a loading control, respectively.

(D) A254 absorption profiles of MBPs. 17 sucrose gradient fractions were collected.

(E) Distribution of mRNAs along the sucrose gradients in (D) as determined by real-time RT-PCR. *AGO1*, *PHB*, *CSD2*, *SPL3*, *SCL6*, and *TCP4* are miRNA target transcripts. *UBQ5*, *eIF4A*, *ACTIN8*, At5g66770, At5g28770, and At2g01570 are nontarget transcripts. The amount of a specific mRNA in each of the 17 fractions is expressed as the percentage of the total amount of the RNA in microsomes. Fractions with negligible amounts of transcripts are not shown.

The error bars represent SD calculated from three biological replicates. *$p < 0.05$; **$p < 0.01$. See also Figure S5.

(Hou et al., 1993), *HAUPTLING* (Jurgens et al., 1991), *MULTIFOLIA* (Lee, 2009), and *PRIMORDIA TIMING* (Mordhorst et al., 1998), to reflect the phenotypes of interest. AMP1 is a homolog of human glutamate carboxypeptidase II, and an active-site glutamate (E) in the human enzyme corresponds to E404 in AMP1, which is mutated to lysine (K) in the *pt* allele of *AMP1* (Figure 4A) (Helliwell et al., 2001). This led to the hypothesis that AMP1 produces an as yet unidentified small molecule that impacts multiple aspects of plant development.

In this study, we uncover a role of *AMP1* and *LAMP1* in miRNA-mediated translation inhibition, but not transcript cleavage. Given that plant miRNAs impact many aspects of plant development, it is not surprising that *amp1* alleles were isolated in a number of genetic screens focusing on various aspects of plant development. The severe developmental defects of the *amp1 lamp1* double mutant suggest that translation inhibition is an essential activity of plant miRNAs. However, it cannot be excluded that *AMP1* and *LAMP1* possess miRNA-independent functions, and these functions contribute to the pleiotropic developmental defects of the *amp1 lamp1* mutant.

EXPERIMENTAL PROCEDURES

Measurement of Protein Synthesis and Protein Half-Life by Metabolic Labeling and Immunoprecipitation

For pulse-labeling-based measurement of protein synthesis, *rdr6 CSD2-HA* and *rdr6 amp1 CSD2-HA* seedlings were incubated in ATS liquid medium containing 800 μCi TRAN ^{35}S-LABEL (MP Biochemicals) for 20 and 40 min. IP was then performed with anti-HA affinity matrix (Roche) to precipitate both labeled (newly synthesized) and nonlabeled (steady-state) CSD2-HA, which were subsequently detected by autoradiography and western blotting, respectively. Pulse-chase experiments were performed to measure the half-life of PHB-MYC. *rdr6 PHB-MYC* and *rdr6 amp1 PHB-MYC* seedlings were incubated in ATS liquid medium containing 1 mCi TRAN ^{35}S-LABEL for 5 hr. After labeling, plants were washed with ATS liquid medium and incubated in ATS liquid medium containing 1 mM methionine/cysteine and 100 μg/ml cycloheximide for 0–3 hr. IP was performed with anti-c-*myc* affinity gel (Sigma).

Isolation and Fractionation of Membrane-Bound Polysomes

To isolate membrane-bound polysomes (MBPs), 2g seedlings were ground in liquid nitrogen, and the powder was suspended in 7 ml microsome extraction buffer (MEB) (see Extended Experimental Procedures). The slurry was filtered with two layers of miracloth and centrifuged at 10,000 × *g* for 15 min at 4°C to remove debris. 100 μl of the supernatant was saved as the total RNA input, and the rest was loaded onto the top of a 2.5 ml 0.6 M/2.5 ml 1.7 M sucrose-step gradient and centrifuged at 140,000 × *g* in a Beckman SW41 rotor for 1 hr at 4°C. The microsome fraction, which sediments to the 0.6 M/1.7 M layer interface, was carefully transferred into a new tube. The microsome fraction was diluted 10 times by MEB and centrifuged at 140,000 × *g* for 0.5 hr to pellet the microsomes. The microsomes were dissolved in 8 ml polysome extraction buffer (PEB) (see Extended Experimental Procedures). Next, sucrose density gradient fractionation was conducted on the microsomes following the same procedure as for total polysomes (Mustroph et al., 2009).

See Extended Experimental Procedures for details on the above-described methods, as well as additional methods and procedures.

SUPPLEMENTAL INFORMATION

Supplemental Information includes Extended Experimental Procedures, five figures, and three tables and can be found with this article online at http://dx.doi.org/10.1016/j.cell.2013.04.005.

ACKNOWLEDGMENTS

We are grateful to Dr. Julia Bailey-Serres for technical advice on polysome profiling. We thank Drs. Kathryn Barton, Nam-Hai Chua, Daniel Kleibenstein, Elliot Meyerowitz, and Zhiyong Wang for sharing plasmids, seeds, or antibodies. We thank Julia Bailey-Serres, Theresa Dinh, Elizabeth Luscher, Kestrel Rogers, and Yuanyuan Zhao for comments on the manuscript. The work was funded by National Institutes of Health (GM061146) and by Howard Hughes Medical Institute and Gordon and Betty Moore Foundation (through Grant GBMF3046) to X.Chen, by the Research Grants Council of Hong Kong (CUHK466610, CUHK466011, and CUHK2/CRF/11G) to L.J., and by National Science Foundation of China to X. Cao and B.M. L.L. was supported by a fellowship from China Scholarship Council.

Received: September 16, 2012
Revised: January 13, 2013
Accepted: March 22, 2013
Published: April 25, 2013

REFERENCES

Aukerman, M.J., and Sakai, H. (2003). Regulation of flowering time and floral organ identity by a microRNA and its *APETALA2*-like target genes. Plant Cell *15*, 2730–2741.

Baumberger, N., and Baulcombe, D.C. (2005). *Arabidopsis* ARGONAUTE1 is an RNA Slicer that selectively recruits microRNAs and short interfering RNAs. Proc. Natl. Acad. Sci. USA *102*, 11928–11933.

Bazzini, A.A., Lee, M.T., and Giraldez, A.J. (2012). Ribosome profiling shows that miR-430 reduces translation before causing mRNA decay in zebrafish. Science *336*, 233–237.

Birckbichler, P.J., and Pryme, I.F. (1973). Fractionation of membrane-bound polysomes, free polysomes, and nuclei from tissue-cultured cells. Eur. J. Biochem. *33*, 368–373.

Brodersen, P., Sakvarelidze-Achard, L., Bruun-Rasmussen, M., Dunoyer, P., Yamamoto, Y.Y., Sieburth, L., and Voinnet, O. (2008). Widespread translational inhibition by plant miRNAs and siRNAs. Science *320*, 1185–1190.

Brodersen, P., Sakvarelidze-Achard, L., Schaller, H., Khafif, M., Schott, G., Bendahmane, A., and Voinnet, O. (2012). Isoprenoid biosynthesis is required for miRNA function and affects membrane association of ARGONAUTE 1 in *Arabidopsis*. Proc. Natl. Acad. Sci. USA *109*, 1778–1783.

Carbonell, A., Fahlgren, N., Garcia-Ruiz, H., Gilbert, K.B., Montgomery, T.A., Nguyen, T., Cuperus, J.T., and Carrington, J.C. (2012). Functional analysis of three Arabidopsis ARGONAUTES using slicer-defective mutants. Plant Cell *24*, 3613–3629.

Chaudhury, A.M., Letham, S., Craig, S., and Dennis, E.S. (1993). *amp1*: A mutant with high cytokinin levels and altered embryonic pattern, faster vegetative growth, constitutive photomorphogenesis and precious flowering. Plant J. *4*, 907–916.

Chen, X. (2004). A microRNA as a translational repressor of *APETALA2* in *Arabidopsis* flower development. Science *303*, 2022–2025.

Chen, J., Li, W.X., Xie, D., Peng, J.R., and Ding, S.W. (2004). Viral virulence protein suppresses RNA silencing-mediated defense but upregulates the role of microRNA in host gene expression. Plant Cell *16*, 1302–1313.

Cikaluk, D.E., Tahbaz, N., Hendricks, L.C., DiMattia, G.E., Hansen, D., Pilgrim, D., and Hobman, T.C. (1999). GERp95, a membrane-associated protein that belongs to a family of proteins involved in stem cell differentiation. Mol. Biol. Cell *10*, 3357–3372.

Conway, L.J., and Poethig, R.S. (1997). Mutations of *Arabidopsis thaliana* that transform leaves into cotyledons. Proc. Natl. Acad. Sci. USA *94*, 10209–10214.

Dalmay, T., Hamilton, A., Rudd, S., Angell, S., and Baulcombe, D.C. (2000). An RNA-dependent RNA polymerase gene in *Arabidopsis* is required for

posttranscriptional gene silencing mediated by a transgene but not by a virus. Cell *101*, 543–553.

Djuranovic, S., Nahvi, A., and Green, R. (2012). miRNA-mediated gene silencing by translational repression followed by mRNA deadenylation and decay. Science *336*, 237–240.

Emery, J.F., Floyd, S.K., Alvarez, J., Eshed, Y., Hawker, N.P., Izhaki, A., Baum, S.F., and Bowman, J.L. (2003). Radial patterning of *Arabidopsis* shoots by class III HD-ZIP and *KANADI* genes. Curr. Biol. *13*, 1768–1774.

Fabian, M.R., Sonenberg, N., and Filipowicz, W. (2010). Regulation of mRNA translation and stability by microRNAs. Annu. Rev. Biochem. *79*, 351–379.

Fukaya, T., and Tomari, Y. (2012). MicroRNAs mediate gene silencing via multiple different pathways in *Drosophila*. Mol. Cell *48*, 825–836.

Gandikota, M., Birkenbihl, R.P., Höhmann, S., Cardon, G.H., Saedler, H., and Huijser, P. (2007). The miRNA156/157 recognition element in the 3′ UTR of the *Arabidopsis* SBP box gene *SPL3* prevents early flowering by translational inhibition in seedlings. Plant J. *49*, 683–693.

Gibbings, D.J., Ciaudo, C., Erhardt, M., and Voinnet, O. (2009). Multivesicular bodies associate with components of miRNA effector complexes and modulate miRNA activity. Nat. Cell Biol. *11*, 1143–1149.

Gibbings, D., Mostowy, S., Jay, F., Schwab, Y., Cossart, P., and Voinnet, O. (2012). Selective autophagy degrades DICER and AGO2 and regulates miRNA activity. Nat. Cell Biol. *14*, 1314–1321.

Goeres, D.C., Van Norman, J.M., Zhang, W., Fauver, N.A., Spencer, M.L., and Sieburth, L.E. (2007). Components of the *Arabidopsis* mRNA decapping complex are required for early seedling development. Plant Cell *19*, 1549–1564.

Helliwell, C.A., Chin-Atkins, A.N., Wilson, I.W., Chapple, R., Dennis, E.S., and Chaudhury, A. (2001). The *Arabidopsis AMP1* gene encodes a putative glutamate carboxypeptidase. Plant Cell *13*, 2115–2125.

Hou, Y., Von Arnim, A.G., and Deng, X.W. (1993). A new class of *Arabidopsis* constitutive photomorphogenic genes involved in regulating cotyledon development. Plant Cell *5*, 329–339.

Jones-Rhoades, M.W., Bartel, D.P., and Bartel, B. (2006). MicroRNAs and their regulatory roles in plants. Annu. Rev. Plant Biol. *57*, 19–53.

Jurgens, G., Mayer, U., Ruiz, R., Berleth, T., and Misera, S. (1991). Genetic analysis of pattern formation in the *Arabidopsis* embryo. Development *113*, 27–38.

Kasschau, K.D., Xie, Z., Allen, E., Llave, C., Chapman, E.J., Krizan, K.A., and Carrington, J.C. (2003). P1/HC-Pro, a viral suppressor of RNA silencing, interferes with *Arabidopsis* development and miRNA unction. Dev. Cell *4*, 205–217.

Kraut-Cohen, J., and Gerst, J.E. (2010). Addressing mRNAs to the ER: cis sequences act up!. Trends Biochem. Sci. *35*, 459–469.

Lanet, E., Delannoy, E., Sormani, R., Floris, M., Brodersen, P., Crété, P., Voinnet, O., and Robaglia, C. (2009). Biochemical evidence for translational repression by *Arabidopsis* microRNAs. Plant Cell *21*, 1762–1768.

Lee, B.H. (2009). Ecotype-dependent genetic regulation of bolting time in the *Arabidopsis* mutants with increased number of leaves. J. Microbiol. Biotechnol. *19*, 542–546.

Lee, Y.S., Pressman, S., Andress, A.P., Kim, K., White, J.L., Cassidy, J.J., Li, X., Lubell, K., Lim, H., Cho, I.S., et al. (2009). Silencing by small RNAs is linked to endosomal trafficking. Nat. Cell Biol. *11*, 1150–1156.

Lerner, R.S., Seiser, R.M., Zheng, T., Lager, P.J., Reedy, M.C., Keene, J.D., and Nicchitta, C.V. (2003). Partitioning and translation of mRNAs encoding soluble proteins on membrane-bound ribosomes. RNA *9*, 1123–1137.

Llave, C., Xie, Z., Kasschau, K.D., and Carrington, J.C. (2002). Cleavage of Scarecrow-like mRNA targets directed by a class of *Arabidopsis* miRNA. Science *297*, 2053–2056.

Mallory, A.C., Dugas, D.V., Bartel, D.P., and Bartel, B. (2004a). MicroRNA regulation of NAC-domain targets is required for proper formation and separation of adjacent embryonic, vegetative, and floral organs. Curr. Biol. *14*, 1035–1046.

Mallory, A.C., Reinhart, B.J., Jones-Rhoades, M.W., Tang, G., Zamore, P.D., Barton, M.K., and Bartel, D.P. (2004b). MicroRNA control of *PHABULOSA* in leaf development: importance of pairing to the microRNA 5′ region. EMBO J. *23*, 3356–3364.

McConnell, J.R., Emery, J., Eshed, Y., Bao, N., Bowman, J., and Barton, M.K. (2001). Role of *PHABULOSA* and *PHAVOLUTA* in determining radial patterning in shoots. Nature *411*, 709–713.

Mordhorst, A.P., Voerman, K.J., Hartog, M.V., Meijer, E.A., van Went, J., Koornneef, M., and de Vries, S.C. (1998). Somatic embryogenesis in *Arabidopsis thaliana* is facilitated by mutations in genes repressing meristematic cell divisions. Genetics *149*, 549–563.

Mourrain, P., Béclin, C., Elmayan, T., Feuerbach, F., Godon, C., Morel, J.B., Jouette, D., Lacombe, A.M., Nikic, S., Picault, N., et al. (2000). *Arabidopsis SGS2* and *SGS3* genes are required for posttranscriptional gene silencing and natural virus resistance. Cell *101*, 533–542.

Mustroph, A., Juntawong, P., and Bailey-Serres, J. (2009). Isolation of plant polysomal mRNA by differential centrifugation and ribosome immunopurification methods. Methods Mol. Biol. *553*, 109–126.

Nelson, B.K., Cai, X., and Nebenführ, A. (2007). A multicolored set of in vivo organelle markers for co-localization studies in *Arabidopsis* and other plants. Plant J. *51*, 1126–1136.

Noll, M., and Burger, M.M. (1974). Membrane-bound and free polysomes in transformed and untransformed fibroblast cells. J. Mol. Biol. *90*, 215–236.

Park, W., Li, J., Song, R., Messing, J., and Chen, X. (2002). CARPEL FACTORY, a Dicer homolog, and HEN1, a novel protein, act in microRNA metabolism in *Arabidopsis thaliana*. Curr. Biol. *12*, 1484–1495.

Peragine, A., Yoshikawa, M., Wu, G., Albrecht, H.L., and Poethig, R.S. (2004). *SGS3* and *SGS2/SDE1/RDR6* are required for juvenile development and the production of trans-acting siRNAs in *Arabidopsis*. Genes Dev. *18*, 2368–2379.

Pillai, R.S., Bhattacharyya, S.N., Artus, C.G., Zoller, T., Cougot, N., Basyuk, E., Bertrand, E., and Filipowicz, W. (2005). Inhibition of translational initiation by Let-7 microRNA in human cells. Science *309*, 1573–1576.

Reid, D.W., and Nicchitta, C.V. (2012). Primary role for endoplasmic reticulum-bound ribosomes in cellular translation identified by ribosome profiling. J. Biol. Chem. *287*, 5518–5527.

Reinhart, B.J., Weinstein, E.G., Rhoades, M.W., Bartel, B., and Bartel, D.P. (2002). MicroRNAs in plants. Genes Dev. *16*, 1616–1626.

Rhoades, M.W., Reinhart, B.J., Lim, L.P., Burge, C.B., Bartel, B., and Bartel, D.P. (2002). Prediction of plant microRNA targets. Cell *110*, 513–520.

Schwab, R., Palatnik, J.F., Riester, M., Schommer, C., Schmid, M., and Weigel, D. (2005). Specific effects of microRNAs on the plant transcriptome. Dev. Cell *8*, 517–527.

Schwartz, B.W., Yeung, E.C., and Meinke, D.W. (1994). Disruption of morphogenesis and transformation of the suspensor in abnormal *sus*pensor mutants of *Arabidopsis*. Development *120*, 3235–3245.

Sunkar, R., Kapoor, A., and Zhu, J.K. (2006). Posttranscriptional induction of two Cu/Zn superoxide dismutase genes in *Arabidopsis* is mediated by downregulation of miR398 and important for oxidative stress tolerance. Plant Cell *18*, 2051–2065.

Tang, G., Reinhart, B.J., Bartel, D.P., and Zamore, P.D. (2003). A biochemical framework for RNA silencing in plants. Genes Dev. *17*, 49–63.

Thermann, R., and Hentze, M.W. (2007). *Drosophila* miR2 induces pseudo-polysomes and inhibits translation initiation. Nature *447*, 875–878.

Vaucheret, H., Vazquez, F., Crété, P., and Bartel, D.P. (2004). The action of ARGONAUTE1 in the miRNA pathway and its regulation by the miRNA pathway are crucial for plant development. Genes Dev. *18*, 1187–1197.

Vazquez, F., Vaucheret, H., Rajagopalan, R., Lepers, C., Gasciolli, V., Mallory, A.C., Hilbert, J.L., Bartel, D.P., and Crété, P. (2004). Endogenous trans-acting siRNAs regulate the accumulation of *Arabidopsis* mRNAs. Mol. Cell *16*, 69–79.

Vidaurre, D.P., Ploense, S., Krogan, N.T., and Berleth, T. (2007). *AMP1* and *MP* antagonistically regulate embryo and meristem development in *Arabidopsis*. Development *134*, 2561–2567.

Won, S.Y., Li, S., Zheng, B., Zhao, Y., Li, D., Zhao, X., Yi, H., Gao, L., Dinh, T.T., and Chen, X. (2012). Development of a luciferase-based reporter of transcriptional gene silencing that enables bidirectional mutant screening in *Arabidopsis thaliana*. Silence *3*, 6.

Xu, J., Yang, J.Y., Niu, Q.W., and Chua, N.H. (2006). *Arabidopsis* DCP2, DCP1, and VARICOSE form a decapping complex required for postembryonic development. Plant Cell *18*, 3386–3398.

Yang, L., Wu, G., and Poethig, R.S. (2012). Mutations in the GW-repeat protein SUO reveal a developmental function for microRNA-mediated translational repression in *Arabidopsis*. Proc. Natl. Acad. Sci. USA *109*, 315–320.